Robotic and Computer Simulated Burrowing Inspired by Mole Crabs

Aakash Parikh

Electrical Engineering and Computer Sciences
University of California at Berkeley

Technical Report No. UCB/EECS-2020-43
http://www2.eecs.berkeley.edu/Pubs/TechRpts/2020/EECS-2020-43.html

May 12, 2020

Acknowledgement

I would like to thank my advisor, Professor Robert Full, for his support and for showing me the value of working collaboratively across fields. I would also like to thank Benjamin McInroe for his mentorship, insights and advice and Professor Ronald Fearing for his help as a reader and for providing valuable feedback on this project. Finally, I would like to thank my family for their endless love and support throughout my education at UC Berkeley.

Robotic and Computer Simulated Burrowing Inspired by Mole Crabs
by Aakash Parikh

Research Project

Submitted to the Department of Electrical Engineering and Computer Sciences, University of California at Berkeley, in partial satisfaction of the requirements for the degree of **Master of Science, Plan II**.

Approval for the Report and Comprehensive Examination:

Committee:

Professor Robert Full
Research Advisor

5/10/20

(Date)

* * * * * * *

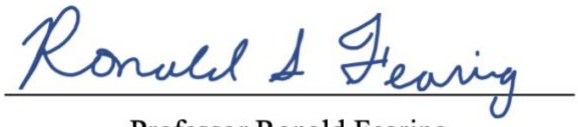

Professor Ronald Fearing
Second Reader

May 10, 2020

(Date)

Abstract

Robotic and Computer Simulated Burrowing Inspired by Mole Crabs

by

Aakash Parikh

Master of Science in Electrical Engineering and Computer Sciences

University of California, Berkeley

Professor Robert Full, Chair

There are a growing number of tasks that require subterranean locomotion and while there are previous studies on burrowing robots, implementing burrowing behaviors in legged robots is a largely unexplored area, due to significant design and control challenges. *Emerita analoga*, the Pacific mole crab, is a natural biological inspiration for developing multimodal legged robotic systems capable of burrowing in granular media. *E. analoga* uses two groups of limbs that expand and excavate substrate to rapidly burrow in intertidal sand. Experiments of physical robots, that leverage design and control principles used by *E. analoga* to burrow, establish the importance of developing limbs that can reduce drag on recovery strokes, and motivate developing a simulation model to quickly model and test parameters. We find that design parameters such as limb lengths have a strong effect on depth reached and the angle of burrowing. Our simulation results also show the importance of coordination between the two limb groups for burrowing and we provide an approximation of a local connection between limb phase and burrowing depth. These results can guide and improve the development of legged burrowing robots. Finally, the simulation environment developed for our experiments is parameterized and configurable to facilitate further study of legged robotic models in granular media.

Contents

List of Figures

Chapter 1

Introduction

Bioinspired design is the idea of looking at biology to spark intellectual thought across all fields and is impactful because of how often Nature's designs are simple and functional [1]. Bioinspired design viewed, more broadly, as design by analogy has many developed pathways to taking ideas from nature and applying them to research [2]. The vast diversity in nature gives us organisms that perform similar tasks to those that we seek to accomplish in robotics. Organisms have evolved various methods of locomotion, such as walking, swimming, flying, climbing and burrowing. They also manipulate objects and their environment, cooperate with others and more. This style of study has sparked various innovations [3, 4, 5].

Distilling these to their core principles can allow us to turn complex biomechanics and behaviors into ideas that we can implement in robotics [6]. Our growing ability to work with new materials increases the scope of possibilities in soft robotics [7]. One such clear application is to use ideas from nature to improve our understanding of burrowing. Burrowing is an ability pervasive in the Animal Kingdom, in which diverse sets of organisms move through granular substrates. This behavior allows animals to escape predators, seek shelter and access food. A robot capable of burrowing in granular media can be essential in circumstances ranging from aiding in emergency situations after ecological disasters, the service and monitoring underground pipes and cables, mining and in transportation.

1.1 Summary of Contributions

This report aims to demonstrate how studying robotic and computer models of the Pacific mole crab, *Emerita analoga*, can help guide the design and control of legged burrowing robots. *Emerita analoga* is an adept burrower, capable of rapidly burrowing into water saturated intertidal sand to filter feed and escape predators. Because the mole crab is capable of rapid burrowing in addition to aquatic and terrestrial locomotion, it provides a natural biological inspiration for developing multimodal legged robotic systems capable of burrowing in granular media.

We briefly discuss the study of control principles of *E. analoga* done by the team at the

UC Berkeley PolyPEDAL lab. This allowed for understanding of control patterns that are robust across burrowing depth and limb loss.

Next, we explore using understanding taken from the crab study on robotic designs for burrowing in granular media. The 3D printed robot is based on a simplification of the mole crab's morphology and includes servo control based on the mole crab's burrowing templates. We discuss current limitations and challenges for such a model and the importance of developing a simulation software to aid in robotic design.

The primary focus of this report is on a simulation software developed to quickly iterate through possible design and control settings for the robotic crab model using principles gleaned from the biological study in our lab. The software is built on the Project Chrono physics engine [8]. This simulation environment is a large N-body granular simulation with a simplified robotic crab model. This simulation allows for a fast (approximately 10 minutes computation time to 5 seconds simulation with 20,000 particles) using a modern CPU to quickly visualize and track body positions and orientations.

Using this simulation software, this report shares analysis of the effect of these parameters on burrowing performance. We begin a simplified model of the physical robot with limb coordination taken from the study of the mole crabs. From this we utilize a design of experiments to identify model parameters that optimize the depth of burrowing into the granular substrate, and develop an approximation of a local connection that relates limb movements to burrowing performance [9, 10].

Moreover, this simulation software is extended to allow for parametrized modification to the environment. The environment allows a user to easily vary substrate parameters including and allows for user definable characteristics for the model. In addition to being used for experiments detailed in this report, the simulation environment can be used as a tool for quickly modelling N-legged motion in granular media.

Chapter 2

Background and Related Work

Granular medium can be characterized as a collection of rigid, macroscopic, non-Brownian particles that primarily interact through friction and collisions. For these particles larger than 1 μm, van der Waals forces, humidity, air drag and thermal agitation are mostly negligible. Granular media exhibits a behavior that is between that of a solid and liquid [11].

Previous work has led to models of granular media for simulations. DEM or Discrete Element Method is a numerical simulation method that can be used to approximate movement of a body through granular media. It assumes that a force on an object is only between particles that touch each other directly and that disturbances do not propagate between particles [12]. For fluidized granular media, Resistive Force Theory (RFT) partitions a body into decoupled segments that generate thrust and experience drag and allows calculation of force using only local properties [13]. A differential complementarity approach takes the Coulomb dry friction model and a non penetration constraint to pose a differential as an optimization problem and calculates velocity based on friction and contact forces, which is used to determine position [14].

Recently, there has been a focus on robotic locomotion on granular media. Using high speed imaging to capture the kinematics of DynaRoACH, and numerical simulation using DEM and multibody simulation, the robot is enabled to run at high speeds on 3mm glass beads [15]. Further examples of robophysics on granular material are reviewed by Goldman et al. including legged locomotion, sidewinding, flipper driven motion and sand swimming [16].

Burrowing through granular media is a behavior of many organisms, in which they move through solid substrate. Burrowing contrasts from other methods such as boring in that they modify the material structure around the burrow through methods such as compaction or excavation [17].

Hosoi and Goldman survey four main regimes of locomotion in granular media based on the relative size of the digger to substrate and speed of motion (inertial number) [18]. The first regime is one with a relatively large ratio of digger to substrate size and a slow motion. This includes undulatory motions found in worms and two anchor diggers such as

clams. A second regime of large relative size and fast motion contains swimmers such as subterraneous snakes. The third regime is one with small relative size and slow motion such as in the roundworm. The fourth regime with a small relative size and fast motion is not known to be found in nature.

There are several examples of burrowing robots developed through bioinspired study across these regimes. Inspired by the Atlantic razor clam, RoboClam studies the contraction speed required to burrow in this method in dry soil [19] and analysis of the cavity by a clam during burrowing created is studied in [20]. A limbless sand swimming robot is designed based on the sandfish, *Scincus scincus*, oscillates to burrow [21]. Based on a mole crab, *Emerita talpoida*, the CRABOT utilizes a deployable vane for the power stroke that folds in recovery and uropods to loosen and displace sand in order to operate in a semi submerged manner [22]. Based on *Paramecium protozoa*, a unicellular ciliate, a robot with a central cavity and multiple cilia like paddles allows for linear translation while submerged in granular substrate [23]. Another such robot is a deformable octahedron robot that takes its inspiration from soft deformable invertebrates, and it can travel through constrained pipes including joints [24].

2.1 *Emerita analoga* Background

Emerita analoga or the Pacific mole crab is a decapod crustacean that ranges up to 35 mm long and 25 mm wide and is found along the sandy beaches of the North American Pacific coast. In order to feed, the mole crab burrows itself into the intertidal sand, and extends two pairs of filter feeding appendages to breathe and to collect food such as phytoplankton [25]. Using anterior legs and rear facing uropods, *E. analoga* can quickly burrow backwards, (tail first), into the soil, excavating the substrate as it digs underground [26].

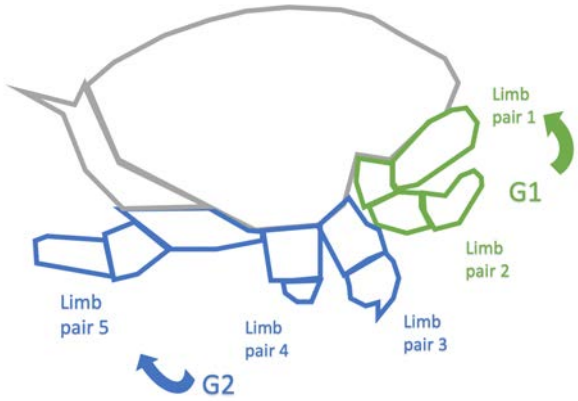

Figure 2.1: Lateral Diagram of *E. analoga* with G1 and G2 highlighted

Studies of the crabs burrowing display an coordinated limb control sequence.With the legs labelled from head to tail as uropod and then limb pairs 2 to 5, shown in Figure 2.1, we see that the limbs are organized into 2 main groups. Group 1 consists of the uropods and second leg pair and Group 2 being pairs 3-5. Group 1 moves with a counterclockwise power stroke, excavating material above the body followed by a clockwise recovery stroke with the appendages folded in. Group 2 rotates in the reverse direction propelling the body forward with a clockwise power stroke followed by a clockwise recovery stroke and excavates material below the body. Furthermore group 1 operates at twice the frequency of group 2, completing twice the amount of strokes in low depths [27].

Results from our lab's study

The UC Berkeley PolyPEDAL lab is studying various aspects of the *Emerita analoga* burrowing behavior [28]. These crabs were studied in a custom made antfarm-like, narrow and transparent tank and were tracked using high speed cameras and analyzed through an automated particle image velocimetry pipeline. The study used a variety of substrates, including natural substrates and index matched Teflon particles to give a clear view into the burrowing patterns of the crab.

Studies from our lab reveal that mole crabs burrow by coordinating several substrate manipulation primitives, including excavation and substrate fluidization. The utilization of these primitives is adaptive to loss of appendages and the depth of the crab in the substrate [29]. For example, the frequency of excavation by G2 limbs generally decreases as the crab transitions from penetrating the substrate to being submerged. However, with restricted uropod (G1) limbs, the G2 limbs compensate, and this frequency of excavation does not decrease [30].

2.2 This Work

Previous studies have developed robots that burrow by peristaltic localized fluidization and fluid injection [31]. However, the implementation of burrowing behaviors in legged robots remains largely unexplored. Legged burrowing presents significant design and control challenges. In order to better understand the design and control challenges involved in legged burrowing, we develop both physical robotic and simulation models of *Emerita analoga* inspired burrowing. Furthermore, we provide a parameterized simulation model that is easily configurable for the study of various legged robotic models in granular media.

Chapter 3

Physical Robotic Model

3.1 Design

Emerita analoga efficiently burrows into sand using its 2 groups of limbs to excavate sand and propel it into substrate. The high dimensional limbs of the crab allow them to alternate between power and recovery stroke, coordinated in templates for burrowing.

A robotic model can take advantage of these coordination templates. However they are also subject to physical limitations such as weight, materials, and motor capabilities. In this chapter, we discuss two designs for burrowing in dry granular media: a model with 4 pairs of limbs that capture both G1 and G2 behavior and a uropod only model with an actuated second degree of freedom.

Single DOF Limbs Octopod Model

The second group of limbs on the crab (G2) helps propel the body deeper into the substrate by excavating material under and behind the crab body. In this model, we develop a robotic model with four pairs of limbs. The first two pairs belong to G1 and excavate material above the robot body, while the third and fourth pairs belong to G2. As limbs can compensate for others within the same group, we reduce the pairs of legs in G2 for simplicity. Without a second DOF to retract limbs on the recovery stroke, we shape the geometry of the limbs to have more drag on the power stroke as compared to the recovery.

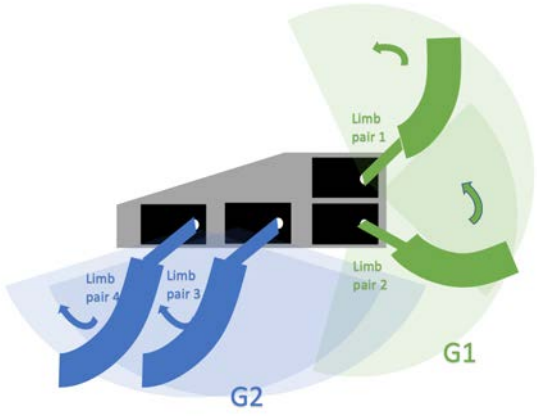

Figure 3.1: Lateral view of physical octopod robot model with single degree of freedom G1 and G2 limbs.

Two DOF Uropod Model

The first group of limbs (G1) excavates substrate above the body of the crab as it burrows during its power stroke. The limbs retract as they return to its original position to prevent undoing the work. This requires a multi degree of freedom limb. In this model, we develop 2 DOF uropods for excavation. The first motor (m1) on the main body allows the limb to be inserted and removed from the substrate, and the second motor (m2) on the limb allows it to sweep forward, excavating the substrate.

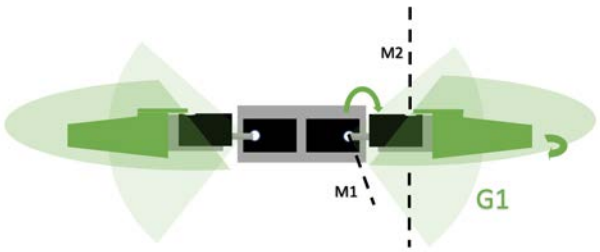

Figure 3.2: Anterior View of physical robot model with two degree of freedom uropods

3.2 Experiments

Setup and Materials

Each of these designs were mocked in a CAD software and 3D printed with PLA plastic. We utilized high torque waterproof SW1210SG digital servo motors from Savox that have 32.0kg/444.4oz-in torque and rotate at 0.13 sec/60 deg at 7.4 volts. Furthermore, a custom control script was written to send PWM signals to the servos using the LynxMotion SSC-32U USB Servo Controller. The motors were powered by an external power supply unit. We designed and fabricated a test bed for the robot using acrylic sheets and used a substrate of uniform plastic beads.

Single DOF Octopod Trials

Combination of G1 and G2 limbs are able to move the robot into the substrate in the first power stroke, however the geometry is unable to sufficiently reduce drag in the recovery phase.

In this experiment, the model was observed as it ran through a series of power and recovery strokes. The limb coordination was as follows: 1) G1 limb excavates substrate counter-clockwise while G1 are in place, 2) G2 limbs excavate substrate clockwise while G1 are in place, 3) G2 returns to its original position, 4) G1 returns to its original position.

These trials show that the first power stroke positions the burrowing head of the robot into the substrate. However, during the recovery stroke the legs move nearly as much substrate as the power stroke negating the movement. Furthermore, when semi-submerged in the granular media, the body pitches forward instead of moving substrate.

Figure 3.3: 3D printed physical robot with 1DOF G1 and G2 limbs, Left: Subject in test bed

G2 angular position during excavation by G1

Results demonstrate that G2 insertion prevents backwards slip during G1 excavation.

This experiment varied the initial angle of the G2 limbs, while the uropods performed a single excavation stroke. Markers on the robot body were tracked by camera to measure displacement from the initial position.

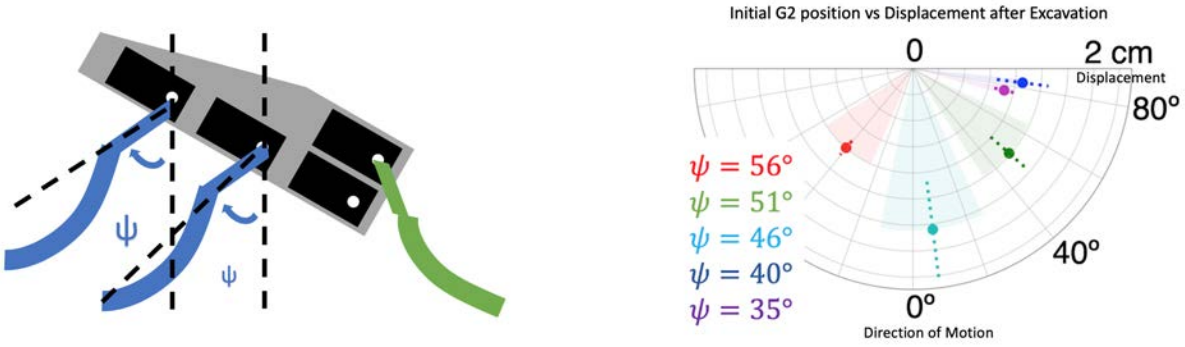

Figure 3.4: Varying of G2 angular position ϕ of 1DOF robot shows that backwards slip measured in in direction θ and magnitude r decreases when limbs are inserted in the substrate

The graph displays the direction and magnitude of motion from an G1 excavation stroke, repeated for various insertion angles (ϕ). For smaller ϕ, when G2 limbs are closer to normal to the surface of the granular media, the displacement is focused in the forward direction. For medium levels of insertion, much of the displacement is directed into the substrate, suggesting a good initial positioning for burrowing. Finally, when G2 is not inserted into the substrate, excavation from G1 causes the robot to slip backwards.

2DOF Uropod Trials

With 2DOF powered limbs, high torque applied on the first motor causes stalling and slippage in M1.

In this experiment we ran trials of running the first cycle of the recovery and power strokes. However, results from these trials were inconclusive as attempting to excavate substrate by moving m2 while m1 has inserted the limb, causes slippage and stalling in m1.

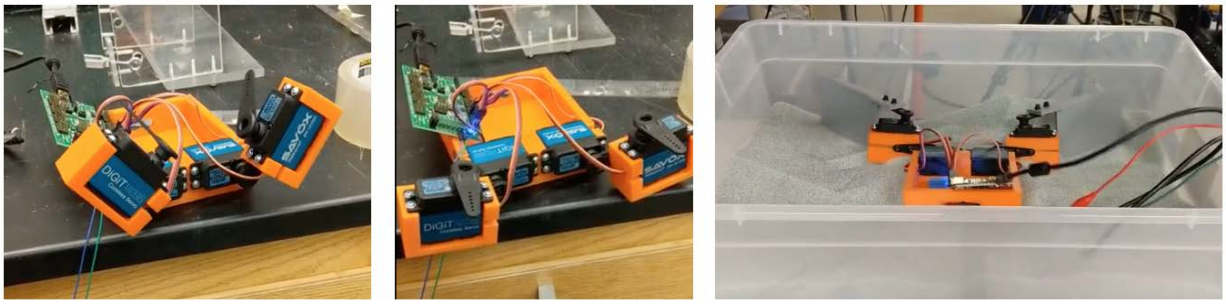

Figure 3.5: 3D printed physical robot with uropods and second powered DOF

3.3 Summary

The largest challenge in designing a robotic model is physical limitations to replicating the high degree of freedom limbs used by the *E. analoga*. This makes it difficult to create a large difference in substrate movement in the power and recovery strokes. By developing a second degree of freedom, we can mitigate this issue, but when submerged in substrate, the forces exerted by the material and heavy complicated limbs can impose significant torque.

Limb to limb and limb to body ratios and other geometrical properties of the robot are impactful in burrowing performance. For example, in trials of the 4 limb pair robot, high G2 limb to body ratios cause pitching of body position rather than excavation of substrate. A physical robot means adjustment of these parameters requires redesign and rebuilding which makes it difficult to rapidly iterate.

Solving these challenges can provide us with a physical robot that utilizes the burrowing primitives exhibited by *E. analoga*. In the next chapter, we discuss a simulation environment that facilitates rapid iterations and testing of robot parameters that can be used to educate modifications to these physical robot designs.

Chapter 4

Computer Simulated Robotic Model

The simulation environment is designed to help us understand the burrowing behavior of the *Emerita analoga* with two main goals in mind: to be able to model key design and control principles derived from the study of the crab and to be able to use the simulation to educate further development of a robotic model.

In order to do so, we provide a simulation environment that allows for modifiable substrate and model parameters and can quickly visualize and assess the effects of these on a modern desktop computer. In this chapter, we discuss the design and functionality of an environment that can do so for a range of legged models and granular medium problems. We design a simplified crab robot model and assess various model and control parameters. We also introduce an approximation of a local connection between the limb rotations and burrowing depth.

4.1 Simulation Environment Design

The simulation environment is built on the Project Chrono physics engine [8]. The environment provides a collision simulation with different shaped objects [32]. We select a complementarity approach to collisions for our analysis but also provide an implementation with a penalty method (Discrete Element Method).

As DEM only considers local collisions, it is ideal for large scale problems, but care must be taken to select a small enough time step to avoid missing collisions [12]. In our analysis, the number of particles is limited by memory required for visualization. The complementarity approach also considers the entire problem, and can be solved with larger time steps between each update.

We choose this instead of an approximation like Resistive Force Theory to model movement in granular media as RFT requires measuring forces by dragging partitions of intruders through the desired substrate [13]. As we seek to be able to modify properties of the medium and intruder we cannot utilize this approach.

If converted to use CPU parallelization/GPU support, simulation can be made faster for a larger number of particles. Utilizing a single core of a modern CPU (i7-9700) a 5 second simulation using 20,000 particles takes approximately 10 minutes using the complementarity approach for collisions.

Expanded Parameterized Design

Our simulation environment is designed to be expandable from this crab model, and allows a wide range of parameterizable input. The design allows modification of size and number of particles and dimensions of the test bed. Material properties of substrate and body can also be adjusted to simulate various kinds of substrate. This includes changing friction coefficients, cohesion values, material density and packing density. Similarly the density and friction of the body material can be adjusted. Additionally, body parameters such as body and limb dimensions, limb speeds, and initial body angle and limb phases can be adjusted.

This allows for a flexible choice of robotic models and experiments on granular media.

Simplified robotic crab model

The crab model designed for this environment takes cues from both the physical robot study and the biological study of the crab. From the physical robot model, we note that high DOF systems are difficult to develop. From biological study, we observe that the burrowing dynamics are adaptive to limb restriction and loss. We first reduce the decapod to a 6 limb model with 1 pair of G1 limbs and 2 pairs of G2 limbs, with simple box geometries. Using a simplified model is important as it allows us to build a flexible platform that can be used to study key design and control parameters.

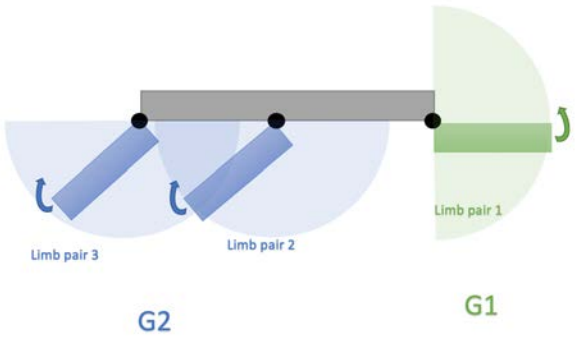

Figure 4.1: Lateral view of simplified model 1DOF-limbed hexapod crab robot model for simulation. Shaded sectors indicate periods where limb interactions occur, during the active power strokes

Since our model has limbs with only a single degree of freedom, a return stroke would have the same resistance as a power stroke, reversing any progress. The mole crab has complex limbs that it retracts towards the body, resulting in greatly reduced resistance in the recovery stroke than in the active stroke. To maintain the single of degree of freedom limb design for the simulation, while reducing the drag on the recovery stroke, we introduce a simplification. Collisions between limbs and the substrate are turned off on the recovery stroke– that is the limb can pass through the substrate without interacting with the particles. This simulates higher degree of freedom appendages. Future work will explore developing higher DOF mechanisms that will interact with particles in return strokes.

4.2 Simulation Experiments and Results

In these experiments we track the position and rotation of the body (at center of mass of the body) over a 6 second simulation. For the 1st second, the crab is stationary, and the substrate is allowed to settle. This is followed by 5 seconds of burrowing. We evaluate burrowing performance as the maximum depth reached (along z axis), and also look at the amount of forward displacement (along y axis). As the body and motion is symmetric, we do not expect any substantial (x axis) movement.

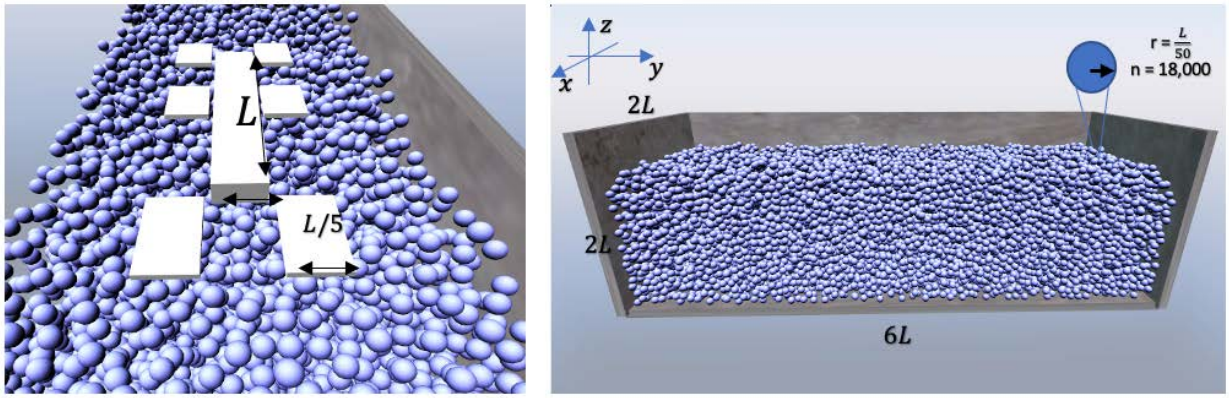

Figure 4.2: Visualization of Simulation Environment. L is the dimensionless length of the crab model and remaining dimensions are relative to body length.

The dimensions used in simulation are in relation to the length of the crab model. The width of the body and of the limbs are one fifth of the body length. We run each of our experiments in a test bed that is 6x2x2 body lengths with 18000 particles with radii 0.02x the size of the body unless specified.

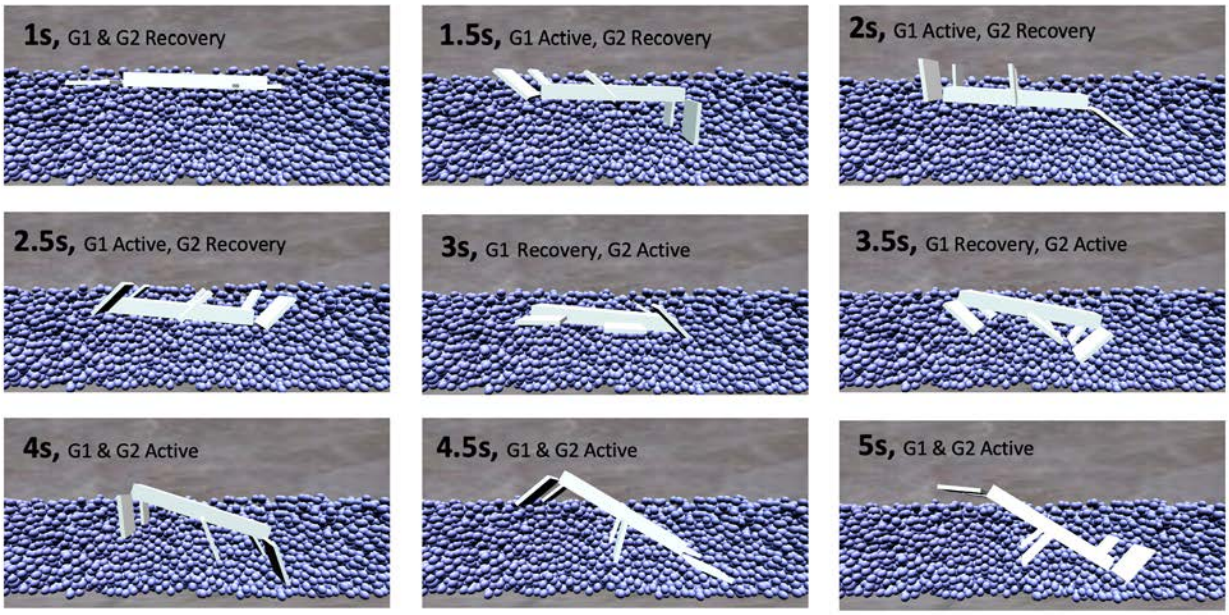

Figure 4.3: Burrowing simulation captured at 0.5s intervals. At each interval, it is indicated whether G1 (right), G2(left, middle) limbs are in recovery or active stages. Some particles are hidden so robot cross section can be seen.

Repeatability Experiment

Experiments are stable over random initializations of substrate positions.

We seek to understand the stability of this simulator. The simulator stochastically generates initial substrate positions within the sandbox, before they settle into place. However, for a given set of parameters, the robot behavior is deterministic. For a randomly selected parameter set, we can run the simulation repeatedly and track the position of the model over time. The figure below displays the results of three randomly selected conditions run 5 times each. The transparent bars indicate the variation in these runs.

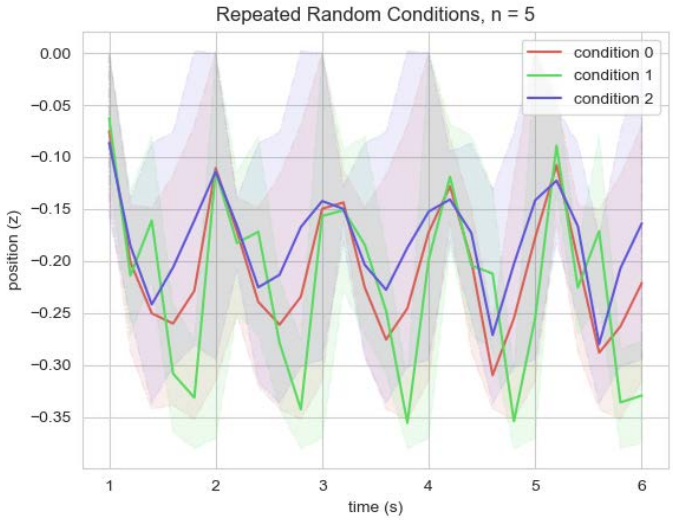

Figure 4.4: Repeated trials with randomly chosen conditions show stable z-position overtime. The solid lines indicate the mean result and the transparent areas show the variation across trials.

Substrate Properties

Variations of substrate material properties including friction, cohesion and particle radius slightly affect burrowing performance.

To assess the results of burrowing in different particle conditions, we set constant values for parameters of the crab model, and individually vary substrate parameters.

The shear strength in granular media comes from both friction and cohesion between particles. By lowering static and kinetic friction, burrowing performance slightly improves, however the difference is negligible. When the material has more friction, the force required to move the material is higher, but the excavated material is slower to reenter. The cohesion value of the substrate has a significant impact. Small values of cohesion allow for burrowing, however, with significant cohesion the performance drastically suffers.

Additionally, the model's ability to burrow is similar across a range of particle sizes. The total volume of the particles was kept constant as the radii changed, and the volume fraction (volume of bounding box of particles / volume of particles) did not change significantly across the trials. This suggests that observations from burrowing in larger particles may carry over to scenarios of burrowing in smaller particles.

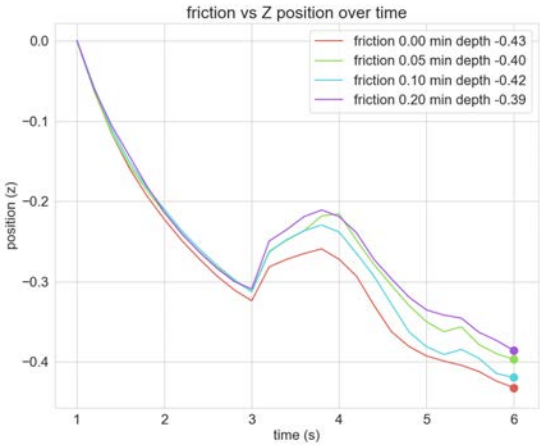

(a) Coefficient of friction is varied and z position of the robot is tracked over time

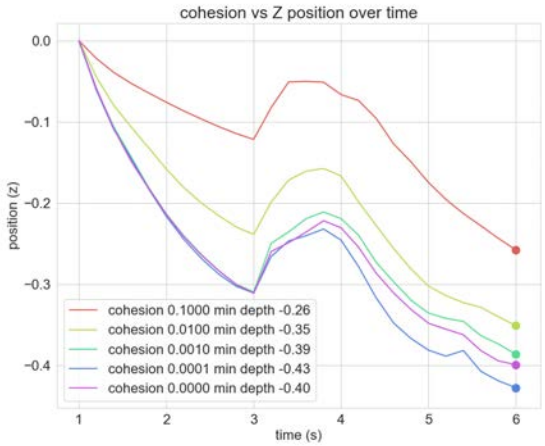

(b) Cohesion between particles is varied and z position of the robot is tracked over time.

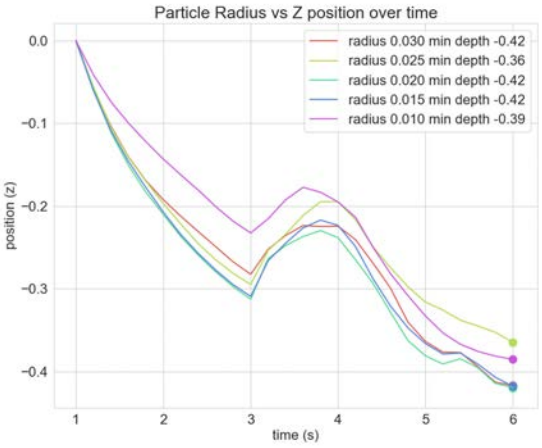

(c) Particle radius is varied and z position of the robot is tracked over time. The number of particles is adjusted to maintain a constant volume.

Figure 4.5: Experimental results of substrate property variations

Model Properties

Limb Speed

Variations in limb speed ratios between G1 and G2 impact in timing and magnitude of burrowing templates. When G1 cycles more frequently than G2 limbs, more motion is concentrated in the downwards (z) direction.

E. analoga cycles G1 at approximately twice the frequency as G2 as it penetrates the substrate. Since we are looking at only the first few cycles of the limb movement, the ratio of G1 to G2 cycles remains constant during each burrow. In each case the fastest limbs were capped to $f = \pi \frac{rad}{s}$ for this experiment.

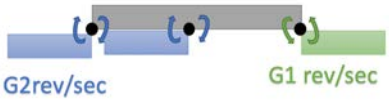

Figure 4.6: Limb speed variation diagram. G2 group limbs move at the same speed

Varying of the relative speeds of the G1 and G2 groups reveals that if the G2 limbs cycle more frequently than G1, the majority of the displacement is along the surface, and the burrow does not penetrate the surface. When G1 cycles more frequently than G2, the magnitude of the motion is correlated with the speed of G2 limbs. As the speeds of G2 decrease compared to G1, the angle of entry increases, but the overall displacement decreases.

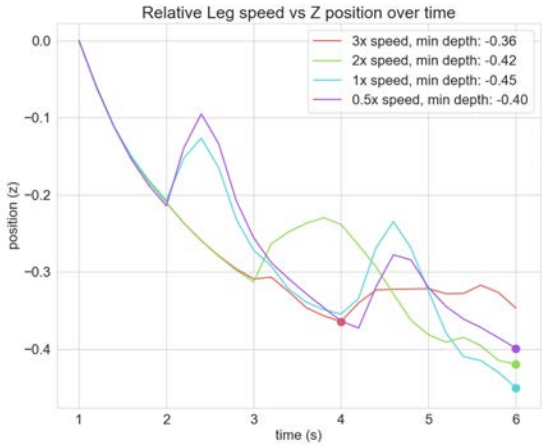

(a) Limb speed ratio between G1:G2 impact z position overtime by changing frequency and length of each phase in burrowing

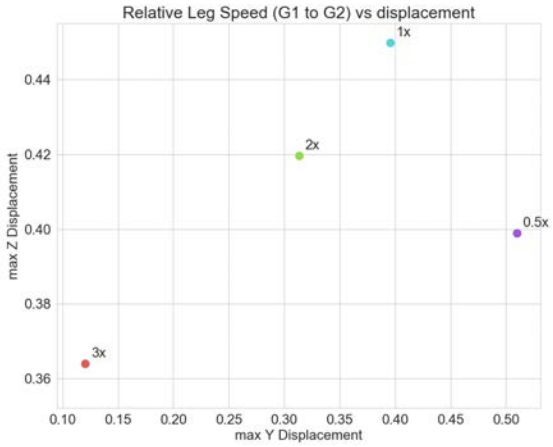

(b) G1:G2 limb speed ratios affect magnitude and direction of displacement along Y, Z axes

Figure 4.7: Experimental results of limb speed variations

Angle of Entry

Variations in initial limb positions can delay the first excavation phase, but result in similar burrowing performance overtime. Steep body angle of entries with leg support results in deeper burrowing, but also in more forward displacement.

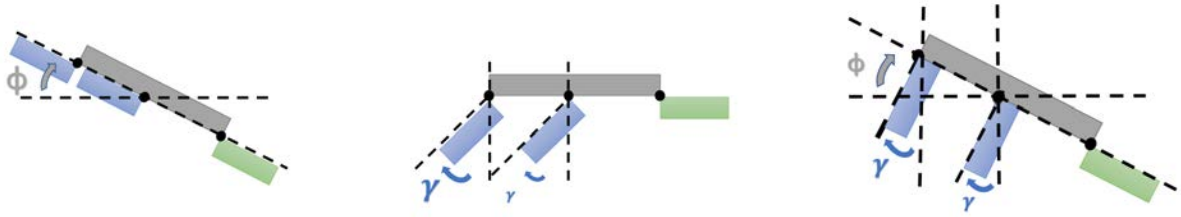

(a) Body Angle Variation- θ indicates initial rotation counter clockwise from parallel to substrate surface

(b) Leg Angle Variation- γ indicates initial rotation counter clockwise from normal to substrate surface

(c) Body Variation with leg support- θ and γ indicate body and leg initial rotations, such that $\theta = \frac{\pi}{2} - \gamma$

Figure 4.8: Angle of entry variations diagrams

Body Angle Variations When the initial body angle is varied while the initial limb positions are held parallel to the body, there is no significant change to the burrowing performance. Without the G2 limbs supporting the body in the angled position, the body falls to the surface of the substrate.

Leg Angle Variations Varying the initial angle on G2 limbs has an effect on when the first excavation phase begins. With deep insertions (small deviation from normal to the surface), we notice a short initial excavation phase, and then a delayed second expansion phase. However, the difference from this on burrowing depth reached is negligible over time.

Body and Leg Angle Variations Initial body angles are varied and are supported by G2 limbs set to be normal to the rotated body. The depth of the body over time is similar to when the limbs are rotated, supporting that limb coordination is responsible for the various phases of burrowing such as excavation. This setting also shows an effect on the direction of motion, and larger body angles result in slightly deeper burrowing, but also cause more forward displacement.

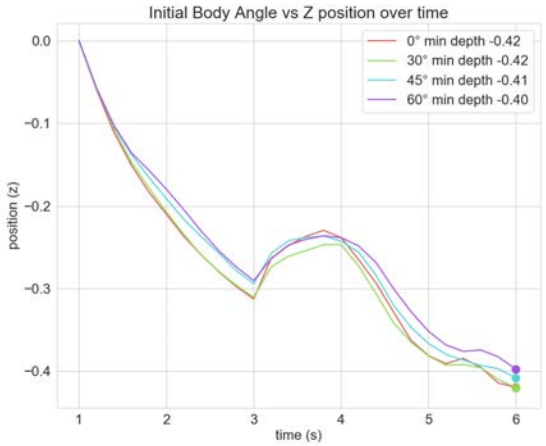

(a) Initial variation of body angle has little impact on z position over time

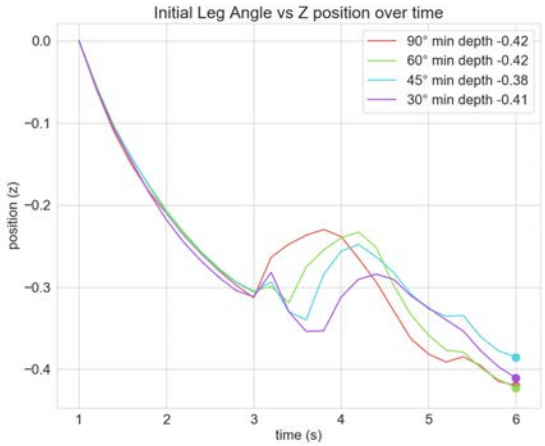

(b) Smaller initial leg angle positions delay upwards slip

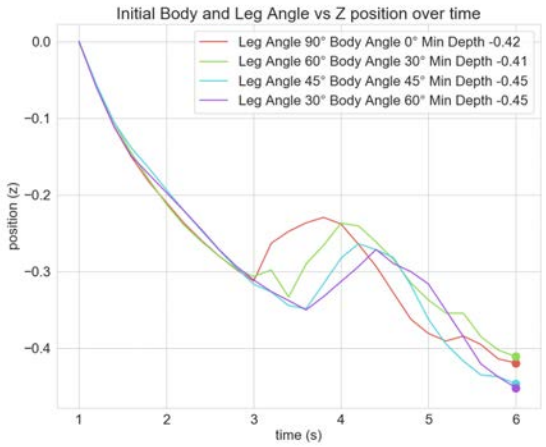

(c) Variations in initial body and leg angles have similar effects as varying leg angles only

(d) Angle of entry variations impact magnitude of displacement but not direction

Figure 4.9: Experimental results of angle of entry variations

Limb length

Deep burrows occur with long G1 limbs, and the combination of long G2 limbs prevents the angle of burrowing from growing shallow.

We search across the space of limb lengths by creating and simulating 40 random initializations, with lengths for each limb pair being selected uniform randomly from (0.05, 0.5). Total G2 limb lengths, $L_{G2} = l_2 + l_1$, where l_2 is not necessarily equal to l_3. G1 total length,

$L_{G1} = l_1$. We group limb sizes into regimes using the total group lengths L_{G1}, L_{G2}. G1 limbs are considered short when $L_{G1} < 0.275$ and are considered long otherwise. G2 limbs are considered short when $L_{G2} < 0.55$ and are long otherwise.

Results from this indicate a strong relationship between overall group lengths and burrowing performance, however, variations within a group do not have a significant effect. Burrowing performance is greatest with long G1 limbs and is improved with long total length G2 limbs. Additionally, we achieve deep burrowing angles when both G1 and total length G2 limbs are short, but the overall magnitude of motion is very small in these cases. The shallowest angles of burrows occur when one group has long limbs and the other has short limbs.

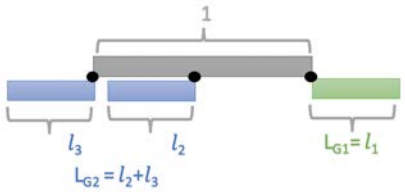

Figure 4.10: Limb length variation diagram

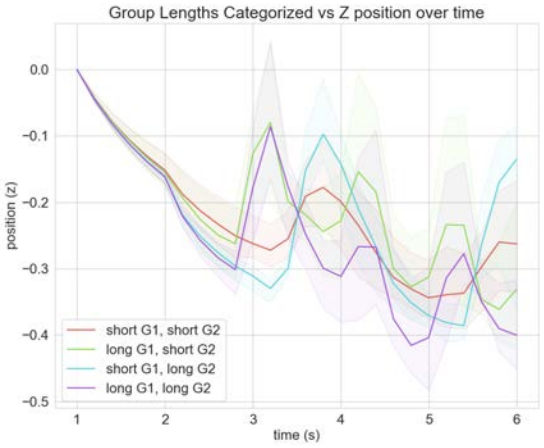

(a) Burrowing patterns over time are similar when placed in regimes by group length, variance is shown by transparent bars

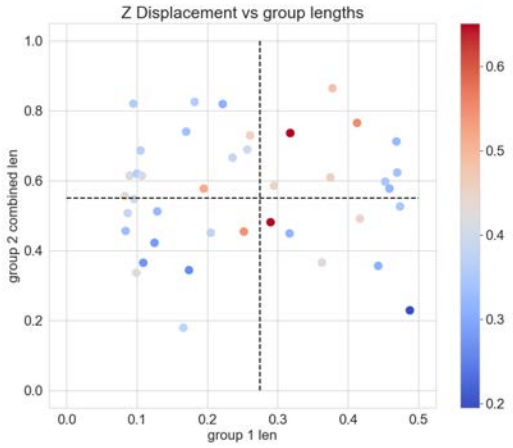

(b) Total group lengths L_{G1}, L_{G2} show areas conducive to burrowing (red) and areas poorly suited (blue)

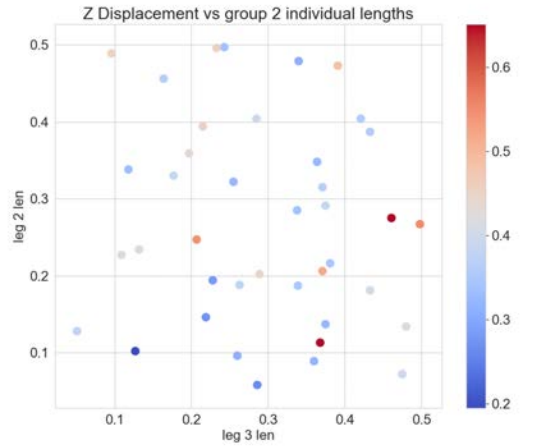

(c) Individual Limb lengths within G2 do not correlate strongly with burrowing performance

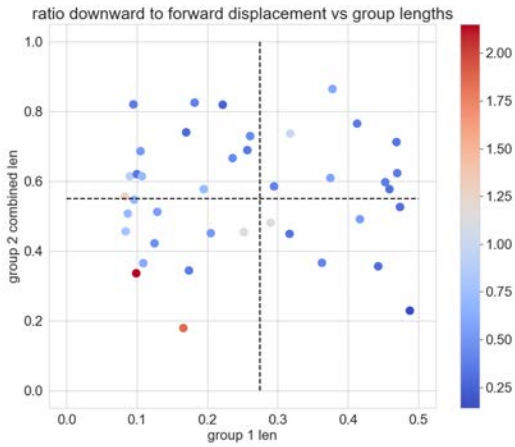

(d) Total group lengths L_{G1}, L_{G2} show areas of downward concentrated motion (red) and forward concentrated areas (blue)

Figure 4.11: Experimental results of limb length variations

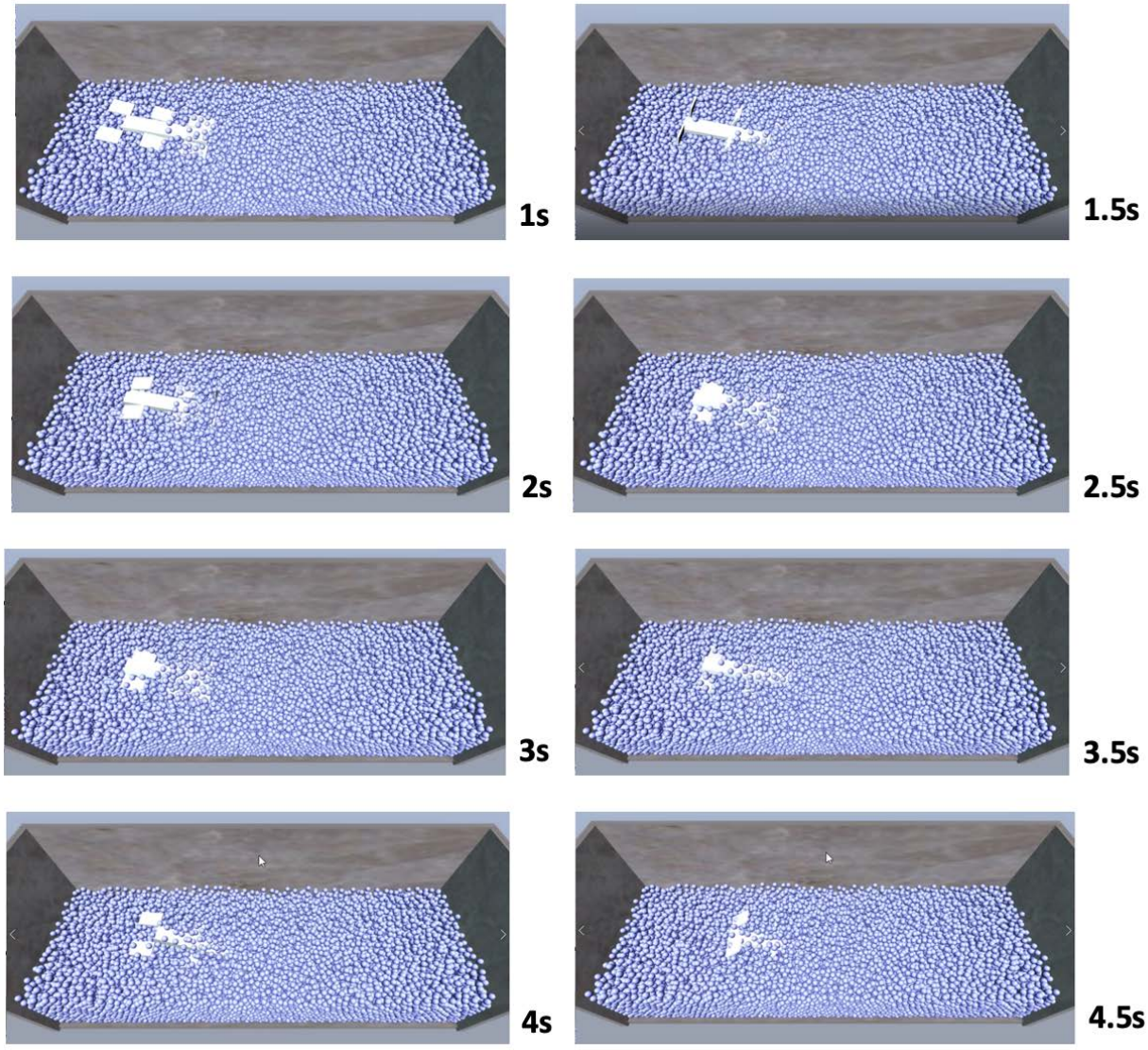

Figure 4.12: Visualization of simulation shows first cycle of burrowing into particles at 0.5s intervals

4.3 Towards Approximating a Local Connection between Limb Phase and Burrowing Depth

A local connection can help explain how changes to the arrangement of the body affects the overall systems position. $A(r)$ maps shape velocities, $\dot{r}$, to body velocities, ξ, represented in the local frame. A local connection specifies this relationship for the entire planning problem.

In a sufficiently constrained system, the behavior is specified by the kinematic reconstruction equation [9, 10].

$$\xi = A(r)\dot{r} \tag{4.1}$$

A local connection can be empirically approximated by sampling configurations r and imposing velocities $\dot{r}$ [33]. We let $r = \phi$, the angular position of the limbs. We can set ϕ to be either ϕ_{G1} or ϕ_{G2}, the angular positions of $G1$ and $G2$ respectively since they are linearly dependant. We are most interested in the vertical burrowing progress, and look at $g = z$.

$$dz = A(\phi)d\phi \tag{4.2}$$

$$A(\phi) = \frac{dz}{d\phi} \tag{4.3}$$

The simulation experimental results demonstrate that model parameters have an effect on the burrow. The relative limb speeds of the groups affects when and how long each burrowing phase occurs, while the group total limb lengths impact the depth and direction of the burrow.

We search across a set of group limb lengths, and repeat these trials with variations of relative limb speeds and for two initial limb configurations shown in Figure 4.13 to approximate the local connection, A, for these parameters. In this experiment, lengths within a group are equal, ie. $l_3 = l_2$ and G1 speeds are kept constant such that $\frac{d\phi_{G_1}}{dt} = \pi \frac{rad}{s}$ for all trials and $\frac{d\phi_{G_2}}{dt} = \frac{\pi}{\alpha} \frac{rad}{s}$. where α is the ratio G1:G2 of limb speeds.

Results from this experiment show that the value of local connection A is correlated with limb phase and is periodic. Each limb group has two main phases: an active power stroke and a recovery stroke. When G1 and G2 limbs move at different speeds, we have four combinations: (Recovery G1, Recovery G2); (Recovery G1, Active G2); (Active G1, Recovery G2); (Active G1, Active G2). In Figure 4.14 these stages are shown in white, blue, green, gray respectively. Figure 4.15 shows how contact forces act upon the limbs in each of these stages.

In an active phase of G1 limbs (green) substrate from the front of the robot is excavated above and behind it. During an active stage of G2 (blue) the robot expands the burrow, initially raising the body and then excavates substrate behind the robot. At the end of this stage and during the recovery stage we see the robot is able to fall deeper into the substrate. This alternation of power and recovery stroke moves the robot deeper into the substrate. When both of the groups are in the same phase, the effect is compounded results in steeper peaks of A. These results are consistent across limb lengths.

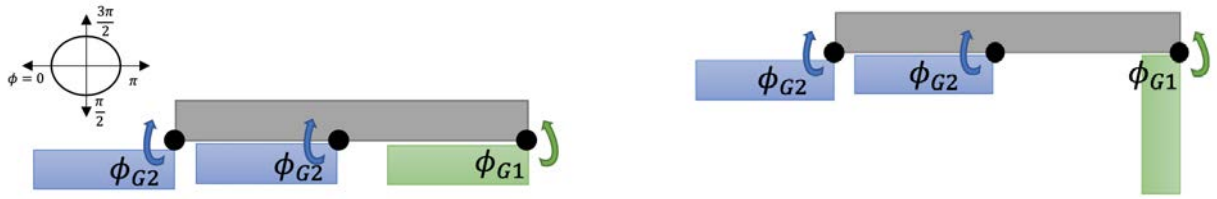

(a) Robot Initial Configuration 1, $\phi_{G1_0}, \phi_{G2_0} = 0$

(b) Robot Initial Configuration 2, $\phi_{G1_0} = \frac{\pi}{2}, \phi_{G2_0} = 0$

Figure 4.13: Diagram of initial configurations for local connection approximation. Configuration 1 begins with G1 in the middle of recovery phase and G2 at the beginning of recovery phase. Configuration 2 begins with G1 in the beginning of active phase and G2 at the beginning of recovery phase.

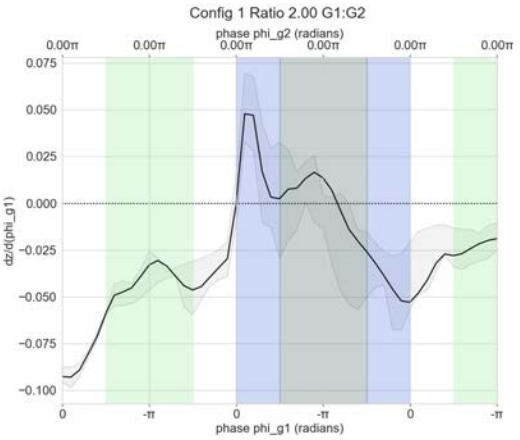

(a) Limb speed of G1 is 2x G2, Config. 1

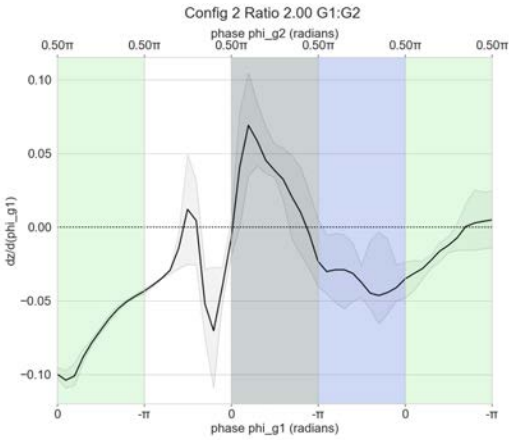

(b) Limb speed of G1 is 2x G2, Config. 2

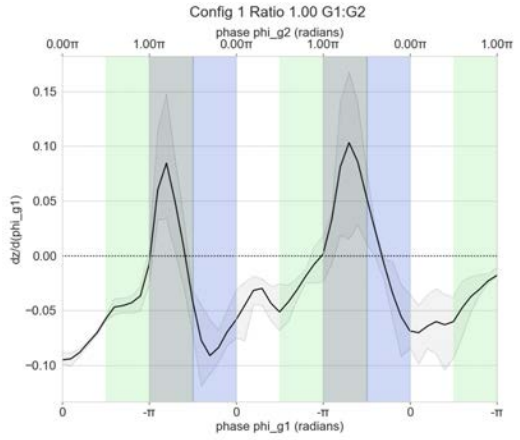

(c) Limb speed of G1 equals G2, Config. 1

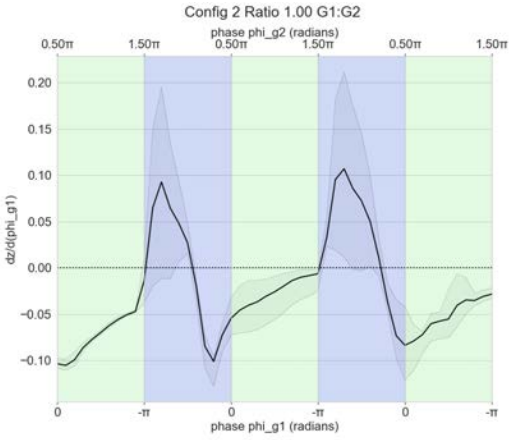

(d) Limb speed of G1 equals G2, Config. 2

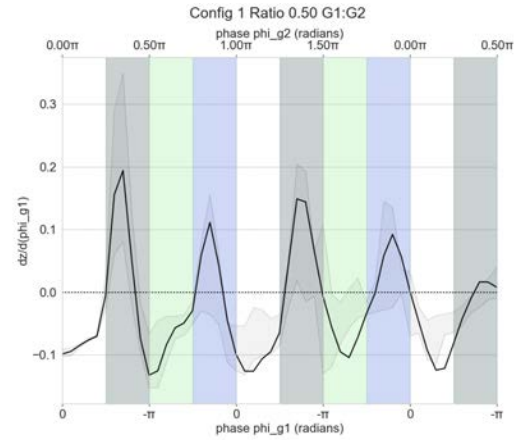

(e) Limb speed of G1 is 0.5x G2, Config. 1

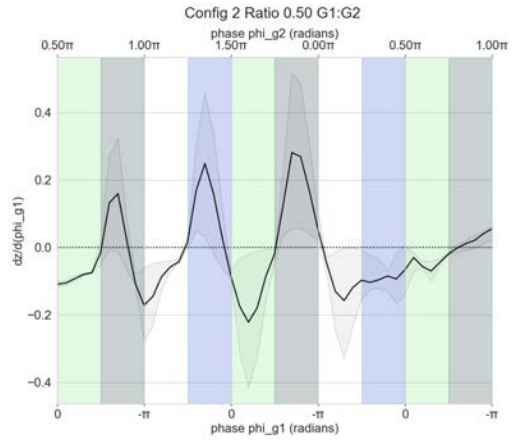

(f) Limb speed of G1 is 0.5x G2, Config. 2

Figure 4.14: Local Connection $A = \frac{dz}{d\phi_{G1}}$ plotted against limb phases for different limb speed ratios. Initial configuration 1 is used in [A,C,E] and initial configuration 2 is used in [B,D,F]. Green vertical bars represent active G1, blue vertical bars represent active G2, and gray bars represent both G1, G2 are active. Variance due to limb lengths are shown in the black error bands.

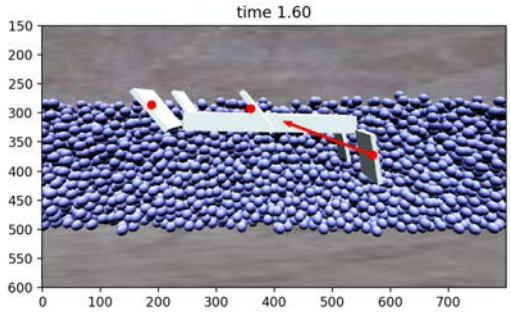

(a) Beginning of active G1 period (Expansion)

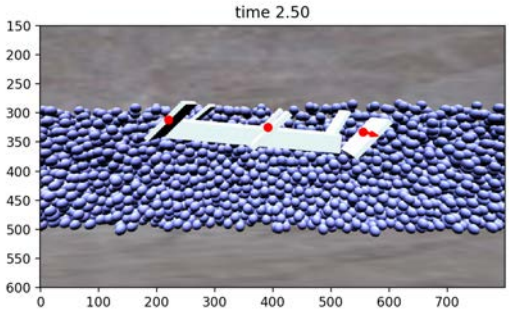

(b) Ending of active G1 period (Excavation)

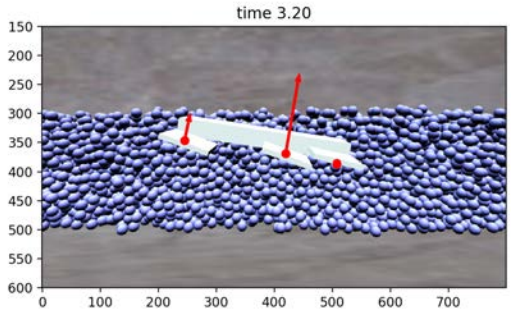

(c) Beginning of active G2 period (Expansion)

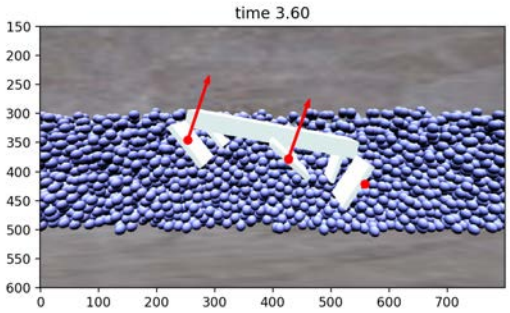

(d) Early middle of active G2 period (Expansion)

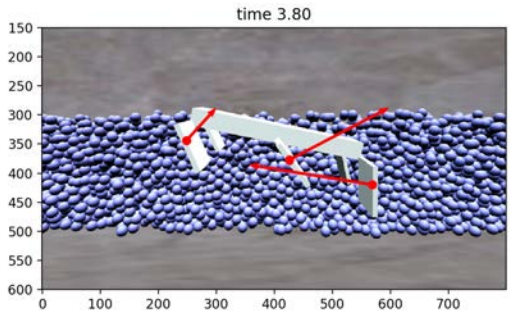

(e) Beginning of G1, Middle of G2 active periods (Expansion)

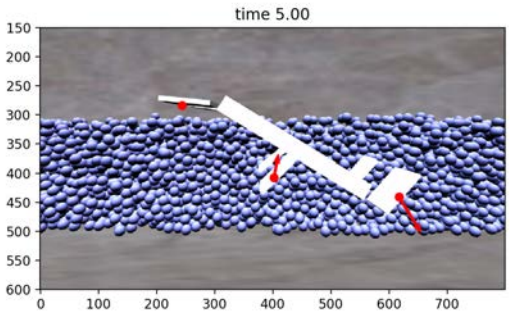

(f) Ending of active G1, Late middle of G2 active periods (Excavation)

Figure 4.15: Forces on limbs show expansion and excavation stages during different phases of an active stroke. Red arrows show net contact forces. When a limb is in recovery, no forces are exerted on the limb. Some particles are hidden to show robot cross section.

4.4 Summary

A simulation environment provides fast visual and numerical feedback for a set of model parameters. Our design using Project Chrono's physics engine allows for rapid testing with different substrate properties and model parameters.

We design a simplified model based on the physical crab robot to assess hypotheses discovered in the biological and physical studies. This hexapod model retains the Group 1 and Group 2 coordination of the mole crab and the physical robot, but assumes that the limbs can be fully retracted (do not contact substrate) in the recovery strokes.

Evaluation of this model showed that variations in the environment and material substrate have minor effects on the burrowing performance. In studying the limb design, relative limb speeds, angle of entry and total limb sizes within a group were found to be important factors in burrowing behavior. The relative limb speeds and angle of entry affect the timing and frequency of upward slips in burrowing. Large G1 limbs are required for burrowing downwards, while large G2 limbs improve the minimum depth reached, and reduce forward displacement of the robot.

We also build an approximation of a local connection between the shape velocities, or the rotation, ϕ, of the limbs, to the z-velocity of the crab robot. This shows a periodic relationship between the phase of limb rotation and the stages in the burrowing process. The active phases begin by expanding the burrow, raising the robot, and then excavate the substrate behind it. This allows the robot to burrow deeper during excavation and continuing into the recovery phase. Upward slips occur when limb are expanding the substrate during active power strokes, and effects are amplified when both limb groups are in the same stage. A model could potentially mitigate the upwards slip by anchoring the robot with the one group's limbs during the other group's active phase.

The results from these experiments can guide further iterations of the physical robot model as well as encourage new areas to look at in our biological studies of *E. analoga*.

Chapter 5

Conclusion

We have presented designs of physical and simulated robots that leverage the burrowing primitives exhibited by *Emerita analoga*. The physical robot designs demonstrate the effectiveness of the G2 limbs in anchoring the crab while excavating, and also show the necessity for increasing the degrees of freedom of the limbs to reduce drag and the amount of substrate moved in the return stroke.

The need to study various configurations and parameters motivated the development a simulation environment. Using a simplified model of the physical 1DOF robot that models both G1 and G2 limbs, we found that key parameters including angle of entry, relative limb speeds and combined limb sizes affect burrowing locomotion. An approximation of a local connection between limb phases and depth of the robot, shows that burrowing progress is periodic due to alternating active and recovery stages that expand and excavate substrate. The results from these simulations can educate designs for a future robot, that can reduce periods of upward slip and maximize downwards progress.

In our experiments, we studied the first few cycles of burrowing, as the robot penetrates the substrate surface. In future studies, we can look at later stages of burrowing. The drag forces in granular media increase linearly with depth [34]. *Emerita analoga*, changes the rates of limb movement as it burrows deeper. Understanding how *E. analoga* overcomes these drag forces and how this translates to a robotic or computer model could reveal techniques to burrow deeper into substrate.

Another future research direction is to investigate how to reduce resistance in the recovery strokes. Our design of a 2DOF robotic model, demonstrated that heavy, actuated limbs experienced large amounts of torque and resulted in motor stalling and slippage. A passive design where the surface area is greatly reduced in the return direction or actuated designs where heavier parts, such as motors, are moved closer to the body may mitigate these limitations.

Our results establish relationships between design and control parameters and burrowing performance using both physical and simulated robotic models inspired by *Emerita analoga*. These findings can be used to guide the development of legged burrowing robots for a wide variety of applications ranging from emergency search and rescue to installing and maintaining

underground infrastructure. Finally, the parameterized simulation environment developed for our experiments is configurable and can be utilized to study N-legged robotic models in granular media.

Bibliography

[1] George M Whitesides. "Bioinspiration: something for everyone". In: *Interface focus* (Aug. 2015). URL: https://www.ncbi.nlm.nih.gov/pmc/articles/PMC4590425/.

[2] Katherine Fu et al. "Bio-Inspired Design: An Overview Investigating Open Questions From the Broader Field of Design-by-Analogy". In: *Journal of Mechanical Design* 136.11 (Oct. 2014). 111102. ISSN: 1050-0472. DOI: 10.1115/1.4028289. eprint: https://asmedigitalcollection.asme.org/mechanicaldesign/article-pdf/136/11/111102/6225652/md_136_11_111102.pdf. URL: https://doi.org/10.1115/1.4028289.

[3] Wolf Thomas et al. "Shape and Deformation Measurement of Free Flying Birds in Flapping Flight". In: *SpringerLink* (Jan. 1970). URL: https://link.springer.com/chapter/10.1007/978-3-642-28302-4_8#citeas.

[4] Selay Yurtkuran, Gözde Kırlı, and Yavuz Taneli. "Learning from Nature: Biomimetic Design in Architectural Education". In: *Procedia - Social and Behavioral Sciences* 89 (2013). 2nd Cyprus International Conference on Educational Research (CY-ICER 2013), pp. 633–639. ISSN: 1877-0428. DOI: https://doi.org/10.1016/j.sbspro.2013.08.907. URL: http://www.sciencedirect.com/science/article/pii/S1877042813030383.

[5] Qiancheng Zhang et al. "Bioinspired engineering of honeycomb structure – Using nature to inspire human innovation". In: *Progress in Materials Science* 74 (2015), pp. 332–400. ISSN: 0079-6425. DOI: https://doi.org/10.1016/j.pmatsci.2015.05.001. URL: http://www.sciencedirect.com/science/article/pii/S0079642515000377.

[6] Rolf Pfeifer, Max Lungarella, and Fumiya Iida. "Self-Organization, Embodiment, and Biologically Inspired Robotics". In: *Science* 318.5853 (2007), pp. 1088–1093. ISSN: 0036-8075. DOI: 10.1126/science.1145803. eprint: https://science.sciencemag.org/content/318/5853/1088.full.pdf. URL: https://science.sciencemag.org/content/318/5853/1088.

[7] Rolf Pfeifer, Max Lungarella, and Fumiya Iida. "The Challenges Ahead for Bio-Inspired "soft" Robotics". In: *Commun. ACM* 55.11 (Nov. 2012), pp. 76–87. ISSN: 0001-0782. DOI: 10.1145/2366316.2366335. URL: https://doi.org/10.1145/2366316.2366335.

[8] Alessandro Tasora et al. "Chrono: An Open Source Multi-physics Dynamics Engine". In: *SpringerLink* (May 2015). URL: https://link.springer.com/chapter/10.1007/978-3-319-40361-8_2.

[9] Ross L Hatton and Howie Choset. "Geometric motion planning: The local connection, Stokes' theorem, and the importance of coordinate choice". In: *The International Journal of Robotics Research* 30.8 (2011), pp. 988–1014. DOI: 10.1177/0278364910394392. eprint: https://doi.org/10.1177/0278364910394392. URL: https://doi.org/10.1177/0278364910394392.

[10] Elie A. Shammas, Howie Choset, and Alfred A. Rizzi. "Geometric Motion Planning Analysis for Two Classes of Underactuated Mechanical Systems". In: *The International Journal of Robotics Research* 26.10 (2007), pp. 1043–1073. DOI: 10.1177/0278364907082106. eprint: https://doi.org/10.1177/0278364907082106. URL: https://doi.org/10.1177/0278364907082106.

[11] Bruno Andreotti, Yoël Forterre, and Olivier Pouliquen. *Granular Media: Between Fluid and Solid*. Cambridge University Press, 2013. DOI: 10.1017/CBO9781139541008.

[12] K. Tanaka et al. "Numerical and experimental studies for the impact of projectiles on granular materials". In: *Handbook of Conveying and Handling of Particulate Solids*. Ed. by A. Levy and H. Kalman. Vol. 10. Handbook of Powder Technology. Elsevier Science B.V., 2001, pp. 263–270. DOI: https://doi.org/10.1016/S0167-3785(01)80028-2. URL: http://www.sciencedirect.com/science/article/pii/S0167378501800282.

[13] Tingnan Zhang and Daniel Goldman. "The effectiveness of resistive force theory in granular locomotion". In: *Physics of Fluids* 26 (Oct. 2014). DOI: 10.1063/1.4898629.

[14] Dan Negrut, Radu Serban, and Alessandro Tasora. "Posing Multibody Dynamics With Friction and Contact as a Differential Complementarity Problem". In: *Journal of Computational and Nonlinear Dynamics* 13.1 (Oct. 2017). 014503. ISSN: 1555-1415. DOI: 10.1115/1.4037415. eprint: https://asmedigitalcollection.asme.org/computationalnonlinear/article-pdf/13/1/014503/6007363/cnd_013_01_014503.pdf. URL: https://doi.org/10.1115/1.4037415.

[15] Tingnan Zhang et al. "Ground fluidization promotes rapid running of a lightweight robot". In: *The International Journal of Robotics Research* 32.7 (2013), pp. 859–869. DOI: 10.1177/0278364913481690. eprint: https://doi.org/10.1177/0278364913481690. URL: https://doi.org/10.1177/0278364913481690.

[16] Jeffrey Aguilar et al. "A review on locomotion robophysics: the study of movement at the intersection of robotics, soft matter and dynamical systems". In: *Reports on Progress in Physics* 79.11 (Sept. 2016), p. 110001. DOI: 10.1088/0034-4885/79/11/110001. URL: https://doi.org/10.1088%2F0034-4885%2F79%2F11%2F110001.

[17] Kelly M. Dorgan. "The biomechanics of burrowing and boring". In: *Journal of Experimental Biology* 218.2 (2015), pp. 176–183. ISSN: 0022-0949. DOI: 10.1242/jeb.086983. eprint: https://jeb.biologists.org/content/218/2/176.full.pdf. URL: https://jeb.biologists.org/content/218/2/176.

[18] A.E. Hosoi and Daniel I. Goldman. "Beneath Our Feet: Strategies for Locomotion in Granular Media". In: *Annual Review of Fluid Mechanics* 47.1 (2015), pp. 431–453. DOI: 10.1146/annurev-fluid-010313-141324. eprint: https://doi.org/10.1146/annurev-fluid-010313-141324. URL: https://doi.org/10.1146/annurev-fluid-010313-141324.

[19] Monica Isava and Amos G. [Winter V]. "Razor clam-inspired burrowing in dry soil". In: *International Journal of Non-Linear Mechanics* 81 (2016), pp. 30–39. ISSN: 0020-7462. DOI: https://doi.org/10.1016/j.ijnonlinmec.2015.12.005. URL: http://www.sciencedirect.com/science/article/pii/S0020746215002395.

[20] Sichuan Huang and Junliang Tao. "Modeling Clam-inspired Burrowing in Dry Sand using Cavity Expansion Theory and DEM". In: *Acta Geotechnica* (Feb. 2020). DOI: 10.1007/s11440-020-00918-8.

[21] Ryan Maladen et al. "Biophysically inspired development of a sand-swimming robot". In: June 2010. DOI: 10.15607/RSS.2010.VI.001.

[22] R. Andrew Russell. "CRABOT: A Biomimetic Burrowing Robot Designed for Underground Chemical Source Location". In: *Advanced Robotics* 25.1-2 (2011), pp. 119–134. DOI: 10.1163/016918610X538516. eprint: https://doi.org/10.1163/016918610X538516. URL: https://doi.org/10.1163/016918610X538516.

[23] R. Andrew Russell. "Comparing Search Algorithms for Robotic Underground Chemical Source Location". In: *Auton. Robots* 38.1 (Jan. 2015), pp. 49–63. ISSN: 0929-5593. DOI: 10.1007/s10514-014-9396-x. URL: https://doi.org/10.1007/s10514-014-9396-x.

[24] Juan Cristobal Zagal, Cristobal Armstrong, and Shuguang Li. "Deformable Octahedron Burrowing Robot". In: July 2012, pp. 431–438. ISBN: 9780262310505. DOI: 10.7551/978-0-262-31050-5-ch057.

[25] *The Pacific Mole Crab: Fact Sheet*. URL: https://limpets.org/wp-content/uploads/2015/01/PacificMoleCrabFS_Oct2010.pdf.

[26] G. E. MacGinitie. "Movements and Mating Habits of the Sand Crab, Emerita analoga". In: *The American Midland Naturalist* 19.2 (1938), pp. 471–481. ISSN: 00030031, 19384238. URL: http://www.jstor.org/stable/2422988.

[27] Zen Faulkes and Dorothy Paul. "Digging in sand crabs (Decapoda, Anomura, Hippoidea): Interleg coordination". In: *The Journal of experimental biology* 200 (Feb. 1997), pp. 793–805.

[28] B McInroe, D Goldman, and RJ Full. "Substrate Volume Fraction Predicts Burrowing Dynamics in Sand Crabs". In: *INTEGRATIVE AND COMPARATIVE BIOLOGY*. Vol. 58. OXFORD UNIV PRESS INC JOURNALS DEPT, 2001 EVANS RD, CARY, NC 27513 USA. 2018, E375–E375.

[29] BW McInroe, A Parikh, and RJ Full. "Mole crabs and a robot reveal control principles for legged burrowing". NSF IWBG Poster. June 2019.

[30] BW McInroe et al. "Reconfigurable control modules enable rapid burrowing in a decapod crustacean". SICB Meeting. Jan. 2020.

[31] Amos G. Winter, Robin L. H. Deits, and A. E. Hosoi. "Localized fluidization burrowing mechanics of Ensis directus". In: *Journal of Experimental Biology* 215.12 (2012), pp. 2072–2080. ISSN: 0022-0949. DOI: 10.1242/jeb.058172. eprint: https://jeb.biologists.org/content/215/12/2072.full.pdf. URL: https://jeb.biologists.org/content/215/12/2072.

[32] Michal Kwarta. "On the Friction and Contact Modeling Methods Used in Simulations of Geomechanical Tests". PhD thesis. University of Wisconsin–Madison, 2017.

[33] Jin Dai et al. "Geometric Swimming on a Granular Surface". In: June 2016. DOI: 10.15607/RSS.2016.XII.012.

[34] P. K. Robertson and R. G. Campanella. "Interpretation of cone penetration tests. Part I: Sand". In: *Canadian Geotechnical Journal* 20.4 (1983), pp. 718–733. DOI: 10.1139/t83-078. eprint: https://doi.org/10.1139/t83-078. URL: https://doi.org/10.1139/t83-078.